Electrochemical and Solid-State Letters, **8** (12) G371-G375 (2005)
1099-0062/2005/8(12)/G371/5/$7.00 © The Electrochemical Society, Inc.

Unassisted Water Splitting from Bipolar Pt/Dye-Sensitized TiO_2 Photoelectrode Arrays

Jong Hyeok Park and Allen J. Bard*,z

Department of Chemistry and Biochemistry, The University of Texas at Austin, Austin, Texas 78712, USA

Direct photodecomposition of water to yield hydrogen and oxygen was achieved with bipolar Pt/dye-sensitized TiO_2 photoelectrode panels, capable of vectorial electron transfer. This novel photoelectrochemical cell, which can overcome the problems of the location of the semiconductor bandedges relative to the water decomposition energy level and the requirement of dye and semiconductor stability during water decomposition in aqueous solution, splits water directly upon illumination without any additional energy input. The maximum hydrogen evolution efficiency of this system, based on the short-circuit current, was 3.7%.
 [DOI: 10.1149/1.2077090]

Manuscript submitted June 15, 2005; revised manuscript received August 4, 2005. Available electronically October 20, 2005.

The direct photodecomposition of water at the inorganic semiconductor/electrolyte interface is not only of scientific interest but also could sustainably produce hydrogen from a solar energy input.[1-3] Solar-to-hydrogen conversion efficiencies of about 12% have been reported for tandem cells based on III/V semiconductors, but these single-crystal materials are too expensive for large-scale terrestrial applications.[4,5]

A key requirement in cells that can make H_2 and O_2 simultaneously with a single semiconductor electrode is the discovery of a semiconductor material that remains stable under irradiation with an appropriate bandgap (>about 2.5 eV) and with a conduction band sufficiently negative for hydrogen evolution and the valence band sufficiently positive for oxygen evolution. The most suitable semiconductors in aqueous solution are oxides, including TiO_2, WO_3, ZnO, and $SrTiO_3$, but the bandgaps of these are so large that the solar efficiency of such cells is very small.[6] Recently, photochemical water splitting by chemically modified n-TiO_2 was described, but the energetics was not suitable for water splitting and required an additional external electrical bias.[7]

To overcome the problems of a large bandgap and inefficient utilization of the solar spectrum, e.g., with TiO_2, dye-sensitizers can be adsorbed on the surface of the electrode or particle.[8] However, a fundamental problem with dye-sensitized systems for oxygen evolution is the photochemical instability of the sensitizer under conditions when holes sufficiently energetic to liberate oxygen from water are produced upon irradiation.[1] Approaches using dye-sensitized solar cells with the iodide/iodine electrolyte for the direct cleavage of water into H_2 and O_2 have been reported.[9] This is based on the external series connection of two different photosystems. The primary disadvantages were the need for external wiring and the stability problem of the semiconductor contacting the water.

During the last decade, a 10.4% light-to-electricity conversion efficiency at air mass 1.5 solar irradiance has been obtained for photovoltaic devices with a panchromatic dye coating nanoporous TiO_2 and a nonaqueous electrolyte containing the iodide/iodine couple in a dye-sensitized solar cell (DSSC).[10] Our group previously described the use of a series array of bipolar TiO_2/Pt and CdSe/CoS photoelectrodes capable of vectorial electron transfer.[11,12] These arrays permitted water splitting to H_2 and O_2 without an additional input of energy. We adopt this same approach here with dye-sensitized solar cells by constructing novel bipolar electrodes, using the iodide/iodine couple in MeCN for internal connections.

We report here the use of two different kinds of cells with bipolar dye-sensitized TiO_2/Pt panels connected so that their photovoltages add to provide vectorial electron transfer for unassisted water splitting to yield the separated products H_2 and O_2 (Fig. 1). Three internal cells (Pt/organic solvent with I^-, I_2 electrolyte/dye-coated TiO_2) behave as photovoltaic cells and the overall photovoltage provides the bias for driving the electrolysis of water at the outer Pt electrodes (acting as the electrode and electrocatalysts for water oxidation to O_2 and reduction to H_2 as shown in Fig. 2). This arrangement overcomes two additional difficulties that are frequently encountered in photoelectrochemical cells, the energetic issue for the reaction and the instability of the semiconductor photoelectrode under conditions where the reaction of interest occurs.

Experimental

Structure A.— A schematic diagram of the structure is shown in Fig. 1A. A 15-nm-thick platinum film was deposited onto one side of a 0.25-mm-thick Ti foil (area: 0.12 cm^2) by sputtering and then a ~15-μm-thick film of TiO_2 nanoparticles [Konarka Technology Inc., (KTI), Lowell, MA] was printed on the back side. After sintering at 450°C for 30 min and cooling to 80°C, the TiO_2-coated Ti foil was dye-coated by immersing it in a 0.3 mM solution of the Ru-dye Z-907 in acetonitrile and *t*-butanol (volume ratio 1:1) at room temperature for 24 h. The end (left) terminal electrode had Pt on both sides. The bipolar and Pt electrodes were inserted into a Pyrex glass tube and attached with a curable epoxy resin (Devcon Co.) at about a 45° angle, with spacing of 1 cm, to allow irradiation of the photoactive sides of the electrodes. All dye-coated TiO_2 regions in the array were in contact with an iodide/iodine electrolyte (0.005 M I_2 + 0.5 M LiI + 0.58 M *t*-butylpyridine in MeCN) and only the two terminal Pt electrodes in contact with aqueous 2 M KOH, connected by a KOH salt bridge.

Structure B.— A schematic diagram of the structure is shown in Fig. 1B. The conducting glass substrate [fluorine-doped tin oxide (FTO) glass, both sides coated] was obtained from Solaronix Co. (Aubonne, Switzerland) and cut into 1 × 1 cm pieces. The front and back sides were connected with a thin film of silver paste. One side of the FTO glass was first cleaned in Triton X-100 solution, then washed with ethanol, and finally treated with an aqueous solution of 50 mM $TiCl_4$ at 70°C for 30 min to make a good mechanical contact between the conducting FTO glass and the TiO_2 layer that would be printed on it. A 15-nm-thick platinum film was deposited onto half of the untreated side of the FTO glass by sputtering and then a ~15-μm-thick film of TiO_2 nanoparticles (KTI) was printed on half of the back side. After sintering at 450°C for 30 min and cooling to 80°C, the TiO_2-coated conducting FTO glass was dye-coated by immersing it into a 0.3 mM solution of the Ru-dye Z-907 in acetonitrile and *t*-butanol (volume ratio 1:1) at room temperature for 24 h. The bottom terminal electrode (right, Fig. 1B) had Pt on both sides, but only one side of the upper end terminal electrode had dye-sensitized TiO_2. The upper terminal (left) FTO glass was connected with a Pt plate to obtain hydrogen. The bipolar and Pt electrodes were inserted into a Pyrex glass tube and attached with a curable epoxy (Devcon Co.) resin, with a spacing of 0.1 cm. To prevent direct contact between cells and water electrolyte, all surfaces except the bottom Pt face were covered with a thin curable epoxy film.

* E-mail: ajbard@mail.utexas.edu
z Electrochemical Society Fellow.

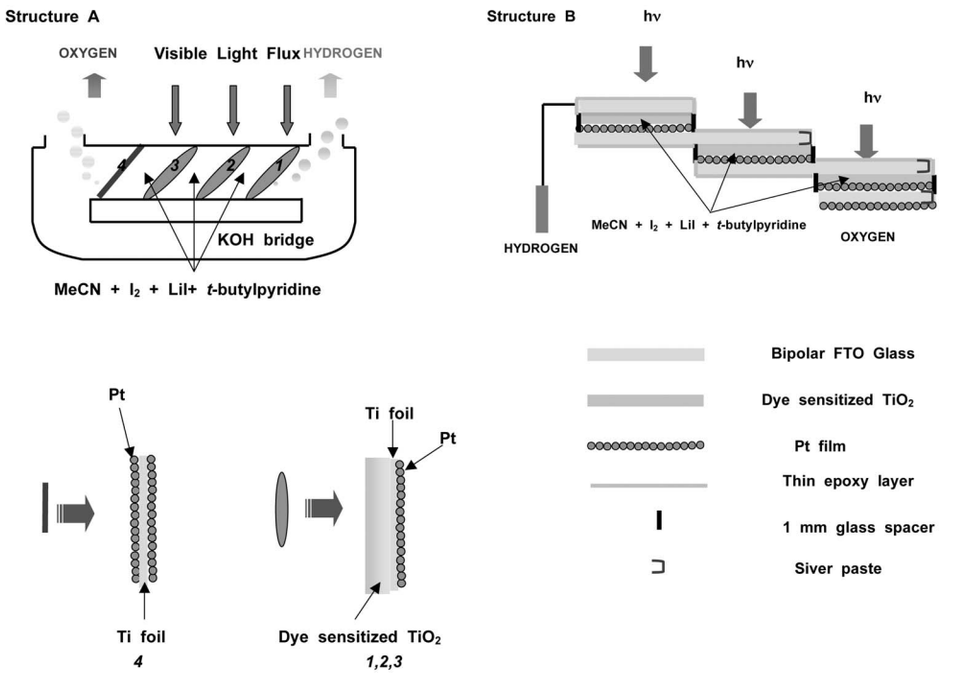

Figure 1. Schematic structure A and B of water photoelectrolysis cells. Expansion shows concrete structure and energetics of bipolar panel.

Light source.— Illumination for the photoelectrolysis was produced by a 2500 W xenon lamp from which infrared wavelengths were removed by an 8 in. water filter. The measured light irradiance was about 100 mW/cm^2.[11]

Results and Discussion

For unassisted water splitting, the internally connected photovoltaic cell must provide sufficient voltage to drive the water redox reactions, i.e., the needed thermodynamic free energy (1.23 V at 25°C), plus additional voltage to overcome kinetic limitations and internal resistive losses.[4] An idealized energy-level diagram for water splitting with this bipolar photoelectrode array (Fig. 2) shows the process, which includes three photons to drive one separated electron-hole pair. When light irradiates the three photoelectrodes, the absorbed photons produce three electron-hole pairs and essentially the same photovoltage, V_1, at each. In these cells, the electrons and holes cause the oxidation of I^- and the reduction of I_3^- in the MeCN. If the resultant photovoltage $V = 3V_1$ is greater than that required for water decomposition for this particular cell structure, H_2 and O_2 evolution at the Pt-deposited Ti foil will occur. Three photons are required to produce one electron in the external circuit, so six photons are required to produce one molecule of H_2.

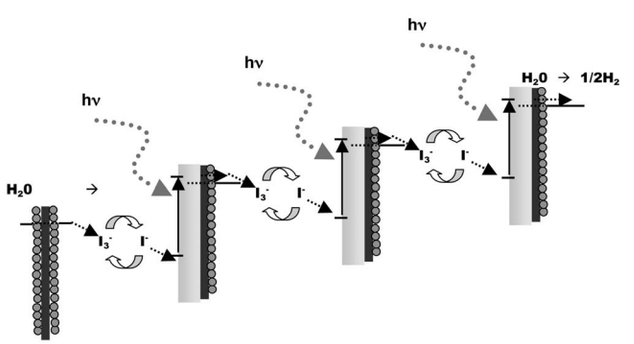

Figure 2. Energy level diagram for the PEC array water splitting device.

The power characteristics of a three-photoelectrode array (structure A) and the spectral distribution of the xenon lamp are shown in Fig. 3. Because the multilayer semiconductor electrode structures involving several photoactive junctions[13] are connected in series, the open circuit photovoltages were additive, yielding about 1.8 V. The fill factor, *FF*, for the series three-cell array was ~0.48.[a] This is smaller than that in the usual DSSC[14-16] because the 1-cm distance between each panel produced a relatively high ionic resistance. The efficiency for electric power generation measured for the three photoelectrode panels was 2.5% as calculated by

$$\eta = V_{oc} i_{sc} FF / P_{in} N$$

where N is the number of photopanels. If a correction is made for the absorption of light by the electrolyte and the effect of the light incident angle (the light flux is directed 45° from the normal to the panels), the efficiency is higher. When the Pt faces contacted aqveous KOH and were connected by a KOH salt bridge, as shown in Fig. 1, bubble formation, presumed to be hydrogen and oxygen, was observed.[b]

The solar to chemical conversion efficiency of the bipolar semiconductor photoelectrochemical (PEC) array was also evaluated by measuring the photocurrent density in the cell shown in Fig. 4, in which the back of the Ti film in bipolar electrode 1 was insulated with epoxy cement and this Ti connected externally through a potentiostat to a Pt gauze electrode.[c] Figure 5 shows photocurrent-voltage curves for this two-electrode configuration. Under illumination at open circuit, the Pt gauze electrode showed a potential of about −400 mV with respect to electrode 1 in the array, indicating

[a]One array means the connecting between ***1*** without back-side Pt film and ***2*** without front-side dye sensitized TiO_2 film. Two array means the connection between ***1*** without back-side Pt film and ***3*** without front-side dye sensitized TiO_2 film. Three array means the connection between ***1*** without back-side Pt film and ***4*** without front-side Pt film.

[b]Chemical reactions pertaining to each interface is; 1,2,3 (front side): $I^- + h^+ \rightarrow I_3^-$; 2,3,4 (back side): $I_3^- + e^- \rightarrow I^-$; 1 (back side): $H_2O + e^- \rightarrow \frac{1}{2}H_2 + OH^-$; 4 (front side): $OH^- + h^+ \rightarrow \frac{1}{4}O_2 + \frac{1}{2}H_2O$. Overall reaction: $\frac{1}{2}H_2O \rightarrow \frac{1}{4}O_2 + \frac{1}{2}H_2$.

[c]The working lead of the potentiostat was connected to the Ti foil of panel ***1*** and the counter and reference lines were connected to the platinum gauze. The KOH electrolyte contacted the left Pt side of panel ***4*** and the platinum gauze.

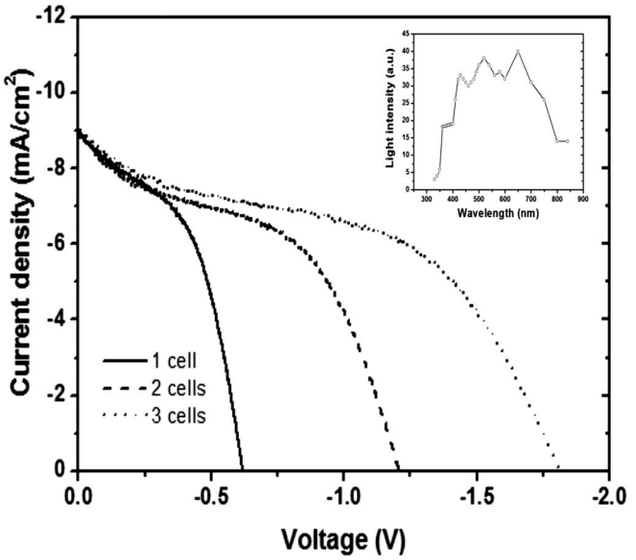

Figure 3. Typical photocurrent density-voltage characteristics of inner photovoltaic cells (structure A) as a function of photoelectrode connection numbers. Effective solar flux: 100 mW/cm^2. Projected area of each panel: 0.12 cm^2. V_{oc}s values are in order from left to right of panel 1 through 3 series. Inset shows the spectral distribution of the xenon lamp.

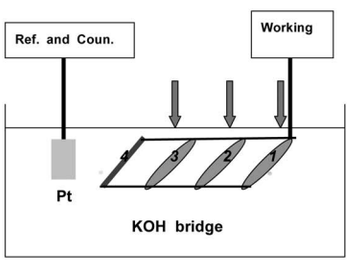

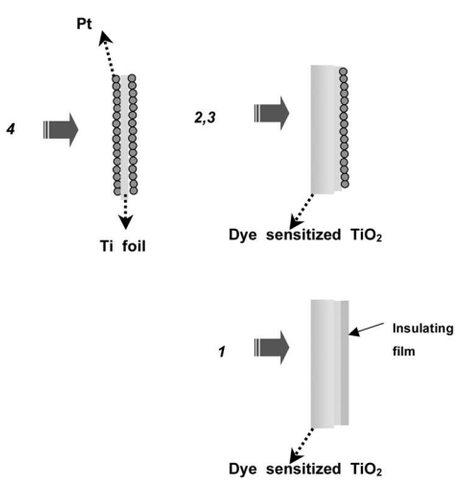

Figure 4. Schematic of the two-compartment electrochemical cell for measuring photocurrent (hydrogen and oxygen production) of photoelectrode PEC array.

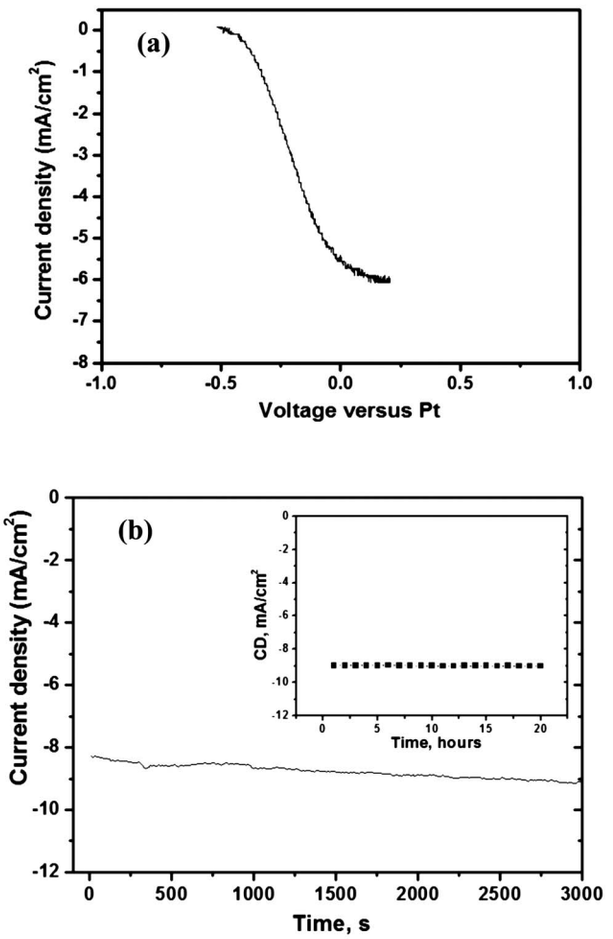

Figure 5. (a) Current density-voltage characteristics for photoelectrode PEC array (structure A) connected by a 2 M KOH bridge under white light illumination. (b) Photocurrent time profile at short circuit for internal photovoltaic cells.

that no additional external voltage was needed for hydrogen generation. At short circuit, the photocurrent density reached 5.4 mA/cm^2. The chemical efficiency during H_2 production was calculated by the following equation: efficiency = (power out)/(power in). The input power is the incident light intensity of 100 mW/cm^2. For the output power, assuming 100% photocurrent electrolysis efficiency, the H_2 production photocurrent of 5.4 mA/cm^2 is multiplied by 1.23 V, which is the standard electrode potential at 25°C.[4] From this equation, the H_2 production efficiency of our system is 2.2%. The value is significant in that this efficiency is realized by a photovoltaic cell with only a 2.5% solar-to-electrical conversion efficiency. Note that solar-to-hydrogen efficiency of the photoelectrode PEC array at zero bias was 88% of the solar-to-electrical conversion efficiency of the inner photovoltaic cell. This means that the maximum operating voltage of the photoelectrode PEC array is very close to that required for electrolysis.[17]

Since only the Pt surfaces of the photoelectrode PEC array are exposed to the aqueous electrolyte, excellent corrosion resistance is expected. In addition, the stability of DSSCs have been improved dramatically, with stable performance under both thermal stress and light soaking matching the durability criteria applied to silicon solar cells for outdoor applications.[18] The internal DSSCs in our system did not show leakage of the MeCN electrolyte into the surrounding aqueous solution and did not need any external leads or internal separators. This suggests that the stability of the internally con-

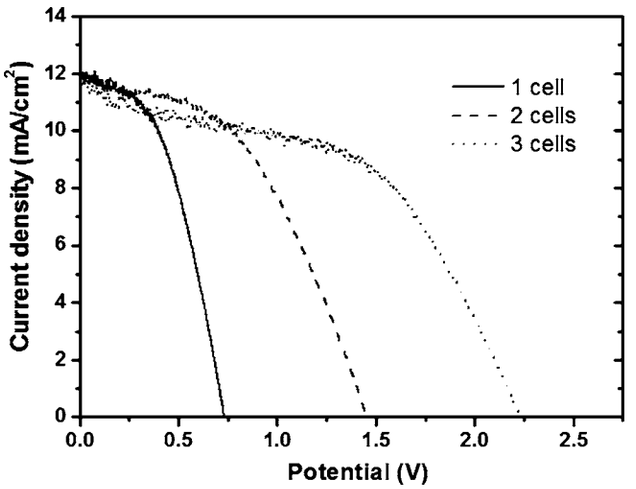

Figure 6. Typical photocurrent density-voltage characteristics of inner photovoltaic cells (structure B) as a function of photoelectrode connection numbers. Effective solar flux: 100 mW/cm^2. Projected area of each panel: 1 cm^2. V_{oc}s are in order from left to right of panel 1 through 3 series.

nected photoelectrode PEC array should be very high. The photocurrent vs time profile for this array under short circuit conditions is shown in Fig. 5b. The current density increased slightly for about 3000 s but then stabilized at about 9 mA/cm^2. The inset in Fig. 5b shows the long-term current stability of the internal connection of the photoelectrode PEC array. After 20 h, the initial current density of 9 mA/cm^2 remained constant, supporting the above hypothesis.

Water splitting characteristics of the photoelectrode PEC array (structure B) were also characterized. The power characteristics of a three-photoelectrode array are shown in Fig. 6. The open circuit photovoltages were also additive, yielding about 2.1 V. The fill factor, *FF*, for the series three-cell array was about 0.52. The efficiency for electric power generation measured for the three photoelectrode panels was 4.5%. Figure 7 shows photocurrent-voltage curves for this two-electrode configuration in a water electrolyte. The H_2 production photocurrent and efficiency was 8.9 mA/cm^2 and 3.7%, respectively. At zero bias (short circuit), copious gas bubbles were seen evolving from both the surface of the bottom terminal electrode and the counter Pt plate. The evolved gases were collected for 30 min. The experimental results in Fig. 8 show the production of

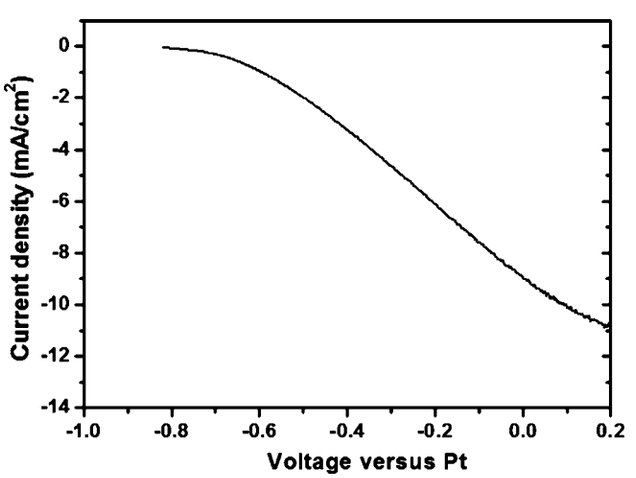

Figure 7. Current density-voltage characteristics for photoelectrode PEC array (structure B) connected by a 2 M KOH bridge under white light illumination.

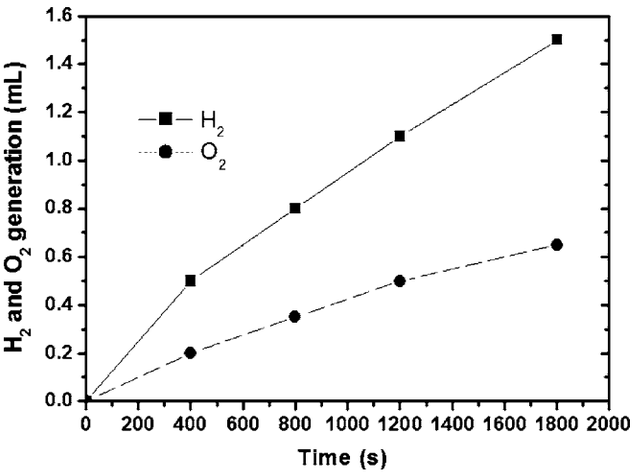

Figure 8. Hydrogen and oxygen photoproduction in a photoelectrode PEC array (structure B).

hydrogen and oxygen occurs with a H_2:O_2 ratio of 2.2:1.

Conclusions

Water can be split into H_2 and O_2 using the bipolar Pt/dye-sensitized TiO_2 photoelectrode panels, capable of vectorial electron transfer, with light as the only energy input. The maximum photocurrent density of the PEC arrays operating at zero bias and a light intensity of 100 mW/cm^2 was 8.9 mA/cm^2 corresponding to a 3.7% light-to-hydrogen conversion efficiency. In these photoelectrode PEC arrays, three photons are required to produce one electron in the external circuit, so six photons are required to produce one molecule of H_2. This is similar to a D4 scheme in III/V semiconductor tandem cells.[19] However, great care needs to be taken in the III/V semiconductor tandem cells to match the photon absorption characteristics so that equal numbers of photocarriers are generated in the top and bottom cells. On other hand, this PEC array can be easily fabricated and may be suited for mass production. Although solar-to-hydrogen efficiency of the PEC array is low compared with that of III/V semiconductor tandem cells, the low cost of the cell materials and possible enhancements in the DSSC efficiencies, make this arrangement an interesting one for further development.

Acknowledgments

Support of this research by the National Science Foundation (CHE 0202136) and fellowship support for J.H.P. by the Korea Research Foundation (grant KRF-2004–214–D00266) is gratefully acknowledged. We thank C. R. Luman for helpful discussions and Dr. Dave Waller, Konarka Technology, Inc., for the TiO_2 and Z-907 samples.

References

1. A. J. Bard and M. A. Fox, *Acc. Chem. Res.*, **28**, 141 (1995).
2. A. J. Bard, *Science*, **207**, 139 (1980).
3. A. Heller, *Science*, **223**, 1141 (1984).
4. O. Khaselev and J. A. Turner, *Science*, **280**, 425 (1998).
5. M. Grätzel, *Nature (London)*, **414**, 338 (2001).
6. G. E. Shakhnazaryan, A. G. Sarkisyan, V. M. Arutyunyan, V. M. Arakelyan A. J. Turner, and R. S. Vartanyan, *Russ. J. Electrochem.*, **30**, 610 (1994).
7. S. U. M. Khan, M. Al-Shahry, and W. B. Ingler, Jr., *Nature (London)*, **297**, 2243 (2002).
8. H. Tributsch and M. Calvin, *Photochem. Photobiol.*, **14**, 95 (1971).
9. J. Augustynski, G. Calzaferri, J. C. Courvoisier, M. Grätzel, and M. Ulmann, in *Proceedings of the 10th International Conference on the Photochemical Storage of Solar Energy, 1994*, p. 229, Interlaken, Switzerland (1994).
10. M. K. Nazeeruddin, P. Pechy, T. Renouard, S. M. Zakeeuddin, R. Humphry-Baker, P. Comte, P. Liska, L. Cevey, E. Costa, V. Shklover, L. Spiccia, G. E. Daecon, C. A Bignozzi, and M. Grätzel, *J. Am. Chem. Soc.*, **123**, 1613 (2001).
11. E. S. Smotkin, A. J. Bard, A. Campion, M. A. Fox, T. Mallouk, S. E. Webber, and J. M. White, *J. Phys. Chem.*, **90**, 4604 (1986).

12. E. S. Smotkin, S. C. March, A. J. Bard, A. Campion, M. A. Fox, T. Mallouk, S. E. Webber and J. M. White, *J. Phys. Chem.*, **91**, 6 (1987).
13. J. R. White, F. F. Fan, and A. J. Bard, *J. Electrochem. Soc.*, **132**, 544 (1985).
14. B. O'Regan and M. Grätzel, *Nature (London)*, **353**, 737 (1991).
15. A. Hagfeldt and M. Grätzel, *Acc. Chem. Res.*, **33**, 269 (2000).
16. M. Gräzel, *Nature (London)*, **414**, 338 (2001).
17. O. O. Khaselev and J. A. Turner, *Electrochem. Solid-State Lett.*, **2**, 310 (1999).
18. P. Wang, S. M. Zakeeruddin, J. E. Moser, M. K. Nazeeruddin, T. Sekiguchi, and M. Grätzel, *Nat. Mater.*, **2**, 402 (2003).
19. J. R. Bolton, S. J. Strickler, and J. S. Connolly, *Nature (London)*, **316**, 495 (1985).